Available online at www.sciencedirect.com
ScienceDirect
International Journal of Heat and Mass Transfer 51 (2008) 1830–1837
International Journal of HEAT and MASS TRANSFER
www.elsevier.com/locate/ijhmt

# Effect of baffle–cavity ratios on buoyancy convection in a cavity with mutually orthogonal heated baffles

P. Kandaswamy [b], Jinho Lee [b], A.K. Abdul Hakeem [a], S. Saravanan [a,*]

[a] UGC-DRS Center for Fluid Dynamics, Department of Mathematics, Bharathiar University, Coimbatore 641 046, India
[b] Department of Mechanical Engineering, Yonsei University, Seoul, Republic of Korea

Received 17 November 2006; received in revised form 16 May 2007
Available online 11 September 2007

**Abstract**

Buoyancy driven convection in a square cavity induced by two mutually orthogonal and arbitrarily located baffles is studied numerically. The baffles are of different sizes and the flow is two-dimensional. The coupled governing equations were solved by finite difference method using Alternating Direction Implicit technique and Successive Over-Relaxation method. The steady state results are presented in the form of streamline and isotherm plots. It is found that buoyancy force plays a key role and overall heat transfer in the cavity is enhanced for higher values of both baffle–cavity ratios. Flow inhibition emerges as a deciding factor and diminishes heat transfer when the horizontal baffle is located above the center of the cavity.


*Keywords:* Natural convection; Buoyancy; Cavity; Heated baffle

## 1. Introduction

Various cooling techniques are currently being used to meet the reliability requirements of micro-electronic components [1]. Among them buoyancy induced natural convection has proved its superiority and has been accepted as a viable alternative to forced cooling in many circumstances. Natural convection provides simple, low-cost, reliable, maintenance free and electronic-interference free cooling. Motivated by the design of modern electronic packages this paper describes natural convection in an air-filled cavity with isothermal walls and two mutually orthogonal heated baffles of different sizes.

Many investigators have studied natural convection in various two-dimensional closed cavities. Simple rectangular cavities with differentially heated vertical walls and adiabatic top and bottom have been examined both theoretically and experimentally for wide ranges of Rayleigh number and aspect ratios [2–6]. Natural convection in cavities with partially active walls has been analyzed by some researchers [7,8]. In general, the aspect ratio and position of the partition play a vital role in the overall heat transfer rate. Ciofala and Karyiannis [9] investigated natural convection in a cavity with partitions protruding centrally from the top and bottom adiabatic walls for different lengths of the partitions. They found that short partitions do not affect the flow pattern but could enhance the heat transfer rate. Frederick and Valencia [10] studied the natural convection of air in square cavity with a diathermal divider for varying lengths and thermal conductivity. Keyhani et al. [11] made an experimental investigation of natural convection in a rectangular cavity with multiple protruding heaters for different aspect ratios. The effect of mounting isothermal fins on the active hot wall was analyzed by Tasnim and Collins [12] and Shi and Khodadadi [13]. They found that the degree of the flow patterns get modified due to blockage of the fin and it augments the overall heat transfer for increasing length of the fin.

* Corresponding author. Tel.: +91 422 2422222x415; fax: +91 422 2425706.
*E-mail address:* sshravan@cycos.com (S. Saravanan).

0017-9310/$ - see front matter © 2007 Elsevier Ltd. All rights reserved.
doi:10.1016/j.ijheatmasstransfer.2007.06.039

**Nomenclature**

| | |
|---|---|
| $A_i$ | baffle–cavity ratios $= 2h_i/L$ |
| $d_1$ | distance between center of cavity and the horizontal plate (m) |
| $D_1$ | dimensionless $d_1$ |
| $d_2$ | distance between center of cavity and the vertical plate (m) |
| $D_2$ | dimensionless $d_2$ |
| $g$ | acceleration due to gravity (m/s$^2$) |
| $Gr$ | Grashof number $= g\beta(\theta_h - \theta_c)L^3/\nu^2$ |
| $h_1$ | height of the horizontal plate (m) |
| $h_2$ | height of the vertical plate (m) |
| $J(\psi,\zeta)$ | Jacobian of $\Psi$, $\zeta$ with respect to $X_1$, $X_2$ |
| $L$ | length of the cavity (m) |
| $Nu$ | local Nusselt number $= \partial T/\partial X_i$ |
| $Nu_{wall}$ | average Nusselt number $= \int_0^1 Nu\, dX_i$ |
| $\overline{Nu}$ | average Nusselt number |
| $Pr$ | Prandtl number $= \nu/\alpha$ |
| $t$ | time (s) |
| $T$ | dimensionless temperature |
| $x_1$ | vertical coordinate (m) |
| $X_1$ | dimensionless vertical coordinate |
| $x_2$ | horizontal coordinate (m) |
| $X_2$ | dimensionless horizontal coordinate |
| $\alpha$ | thermal diffusivity of fluid (m$^2$/s) |
| $\beta$ | volumetric coefficient of expansion of fluid (1/K) |
| $\theta$ | temperature (K) |
| $\psi$ | stream function (m$^2$/s) |
| $\mu$ | dynamic viscosity of fluid (Pa s) |
| $\nu$ | kinematic viscosity of fluid $= \mu/\rho$ (m$^2$/s) |
| $\rho$ | density of fluid (kg/m$^3$) |
| $\tau$ | dimensionless time |
| $\omega$ | vorticity (1/s) |
| $\Psi$ | dimensionless stream function |
| $\zeta$ | dimensionless vorticity |

*Subscripts*

| | |
|---|---|
| c | cold |
| h | hot |
| $i$ | 1, 2 |
| B | bottom |
| L | left |
| R | right |
| T | top |

Another problem of interest is to extract heat from hotter bodies contained in closed cavities. Oztop et al. [14] have addressed such an issue with a thin heated plate built in vertically or horizontally and found that heat transfer is enhanced by about 20% when the plate is located vertically. Dagtekin and Oztop [15] have dealt with the heat removal from two heated vertical partitions of different heights placed on the bottom of a cavity and observed the enhancement of heat transfer with an increase in spacing between the two partitions and also increase in the height of the partitions.

Both cavity–chip and chip–chip aspect ratios play vital role in modeling the optimal heat exchangers and electronic packaging design. Heat transfer in an enclosure with two mutually orthogonal heated plates has received limited attention though such configurations are encountered in microelectronics industry. Papanicolaou and Jaluria [16] and Icoz and Jaluria [17] have considered such cases in their design and optimization of cooling systems for electronic equipments. Having this in mind natural convection in a square cavity induced by two mutually orthogonal heated plates has been recently studied by the authors [18]. This paper extends the above study when the two plates are of different sizes.

## 2. Mathematical analysis

The square cavity of length $L$ under consideration is shown schematically in Fig. 1. It contains two isothermally heated horizontal and vertical thin baffles of lengths $h_1$ and $h_2$, respectively. The horizontal and vertical baffles are at distances $d_1$ and $d_2$ from the center $O$ of the cavity. All the four walls of the cavity are isothermally maintained at a constant temperature $\theta_c$, which is lower than that of the baffles. The cartesian co-ordinates $(x_1, x_2)$ with the corresponding velocity components $(v_1, v_2)$ are chosen. The gravity $g$ acts downwards normal to the $x_2$ direction.

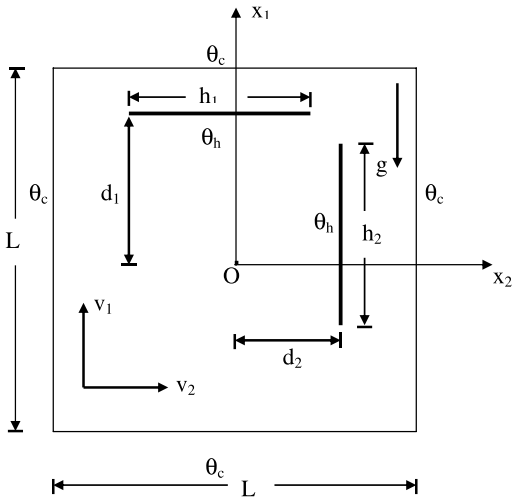


Fig. 1. Physical configuration.

The nondimensional equations governing the laminar two-dimensional incompressible flow of the fluid under

Boussinesq approximation in an environment described above are

$$\frac{\partial\zeta}{\partial\tau}+J(\psi,\zeta)=Gr\frac{\partial T}{\partial X_2}+\nabla^2\zeta \tag{1}$$

$$\frac{\partial T}{\partial\tau}+J(\psi,T)=\frac{1}{Pr}\nabla^2 T \tag{2}$$

$$\nabla^2\psi=-\zeta \tag{3}$$

with the initial and boundary conditions

$$\begin{aligned}&\tau=0;\quad \frac{\partial\psi}{\partial X_2}=\frac{\partial\psi}{\partial X_1}=0;\quad T=0;\\ &\text{at}\ -\frac{1}{2}\leqslant X_1\leqslant\frac{1}{2};-\frac{1}{2}\leqslant X_2\leqslant\frac{1}{2}\\ &\tau>0\quad \frac{\partial\psi}{\partial X_2}=\frac{\partial\psi}{\partial X_1}=0\quad T=0;\quad \text{at}\quad X_1=\pm\frac{1}{2};X_2=\pm\frac{1}{2}\\ &\frac{\partial\psi}{\partial X_2}=\frac{\partial\psi}{\partial X_1}=0\quad T=1\ \text{on the baffles}\end{aligned} \tag{4}$$

The dimensionless variables are defined as $X_1=x_1/L$, $X_2=x_2/L$, $\tau=tv/L^2$, $T=(\theta-\theta_c)/(\theta_h-\theta_c)$, $\Psi=\psi/v$ and $\zeta=\omega L^2/v$. The nondimensional parameters appearing in the above equations are the Grashof number $Gr=g\beta(\theta_h-\theta_c)L^3/v^2$ and the Prandtl number $Pr=v/\alpha$. In order to measure heat transfer rate in the cavity, it is necessary to define wall Nusselt numbers at the four walls as $Nu_{wall}=\int_{-0.5}^{0.5}Nu\,dX_i$, where the local Nusselt number $Nu=\frac{\partial T}{\partial X_i}$. The average Nusselt number $\overline{Nu}$ is then calculated by averaging the wall Nusselt numbers at the four walls. If one of the baffles lies on a cavity wall, only the remaining part of that wall is taken into account in calculating $Nu_{wall}$. In addition to these, we define two nondimensional numbers $A_1=2h_1/L$ and $A_2=2h_2/L$ to study the influence of relative sizes of the horizontal and vertical baffles with respect to the cavity.

The equations are solved numerically using finite difference method with a regular and uniform cartesian space grid. The grid is chosen in such a way that the thin baffles coincide with the grid points. An Alternating Direction Implicit technique and Successive Over-Relaxation method are employed to solve the discretized equations as reported in [4]. The results obtained by the code developed were validated against those of Zhong et al. [3] and Oztop et al. [14] (see Fig. 2b). In order to determine a proper grid size for this study, a grid independency test was conducted for $Gr=10^6$, $Pr=0.71$, $A_1=A_2=0.5$ and $D_1=D_2=0$. Five different grids $41\times41$, $61\times61$, $81\times81$, $101\times101$ and $121\times121$ were chosen. The maximum value of the stream function of the primary vortex ($\Psi_{max}$) was used as a sensitivity measure of the accuracy of the solution. Fig. 2a shows that the two grids $101\times101$ and $121\times121$ give nearly identical results. Hence considering both the accuracy and the computational time, the computations were all performed with a $101\times101$ grid.

## 3. Results and discussion

A numerical analysis was made to predict natural convection arising in a square cavity due to two mutually orthogonal heated baffles of different sizes. The computations were carried out with $Pr=0.71$, corresponding to air and $Gr=10^6$. We fixed $h_1$ and $h_2$ to be half of the cavity length while varying $A_2$ and $A_1$, respectively. When $D_2=0$, the problem is symmetrical about $X_2=0$ and hence in this case we have plotted both the isotherms and streamlines in a single plot. Fig. 3 shows the temperature distributions and flow patterns for the cases when either a vertical ($A_1=0$) or horizontal ($A_2=0$) baffle is placed at the center of the cavity. These clearly indicate two counter rotating moderate convection cells both rising at the center of the cavity. It should be noted that when $A_2=0$ each cell has a stronger primary eddy above and a secondary weaker one below the baffle. We find that the heat transfer rate is more for the case $A_1=0$ compared to $A_2=0$, in agreement with the observation of Oztop et al. [14]. We study

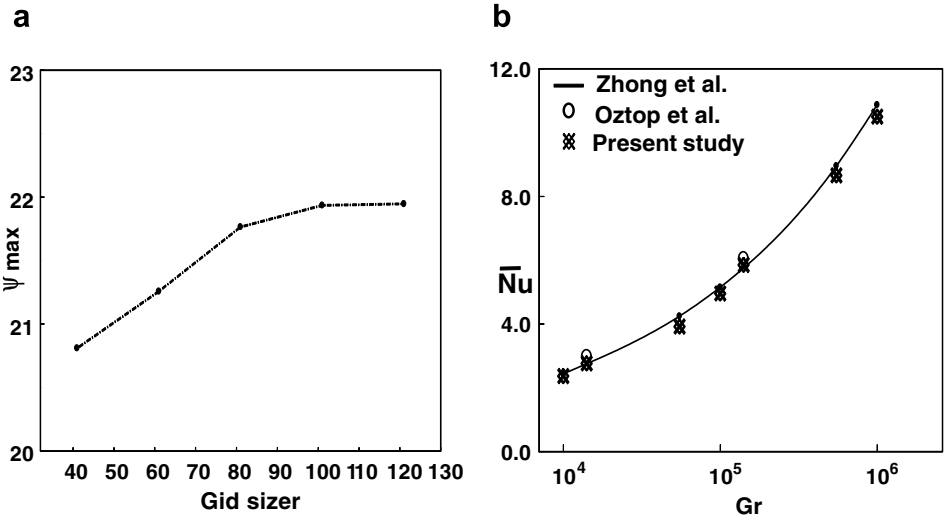


Fig. 2. (a) $\psi_{max}$ as a function of the grid size and (b) correlation of present numerical results with others.

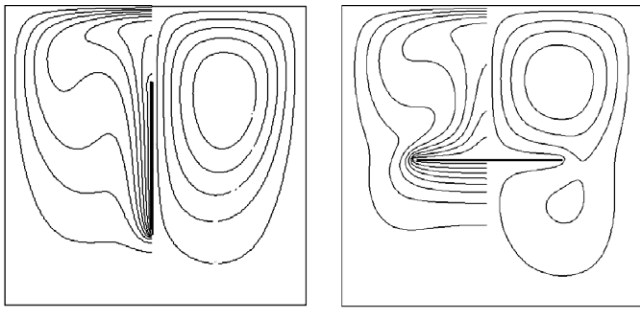


Fig. 3. Isotherms and streamlines for $A_1 = 0$ and $A_2 = 0$ (a) $\Psi_{\max} = 22.7903$ and (b) $\Psi_{\max} = 19.1984$.

the effects of $A_1$ and $A_2$ by keeping $D_2 = 0$ and $D_1 = 0$, respectively.

The isotherms and streamlines for different values of $A_1$ are shown in Fig. 4 keeping $D_2 = 0$. When $D_1 = 0$ an increase in $A_1$ from 0.5 to 1.0 starts dividing the counter rotating cells into primary eddies at the top and secondary ones at the bottom of the cavity. Further increase in $A_1$ to 1.5 completely divides the cells and results in a pair of strong counter rotating cells at the upper half of the cavity and another pair of weak counter rotating cells at the bottom of the cavity. When $D_1 = 0.25$ an increase in the length of the horizontal baffle pushes the primary eddies slightly below and ultimately results in a pair of counter rotating cells below the heated baffle and a pair of small and weaker cells near the top of the cavity. But in the case of $D_1 = -0.25$, the cells are pushed above the horizontal baffle and the transport in the fluid below the baffle is conduction-dominated. We found no significant change in the flow characteristics for the extreme wall mounted cases $D_1 = 0.5$ and $-0.5$ except the change in $\overline{Nu}$ and hence they are not displayed.

When $D_1 = 0$, the problem is anti-symmetric about $X_2 = 0.0$. Hence we have considered only positive values

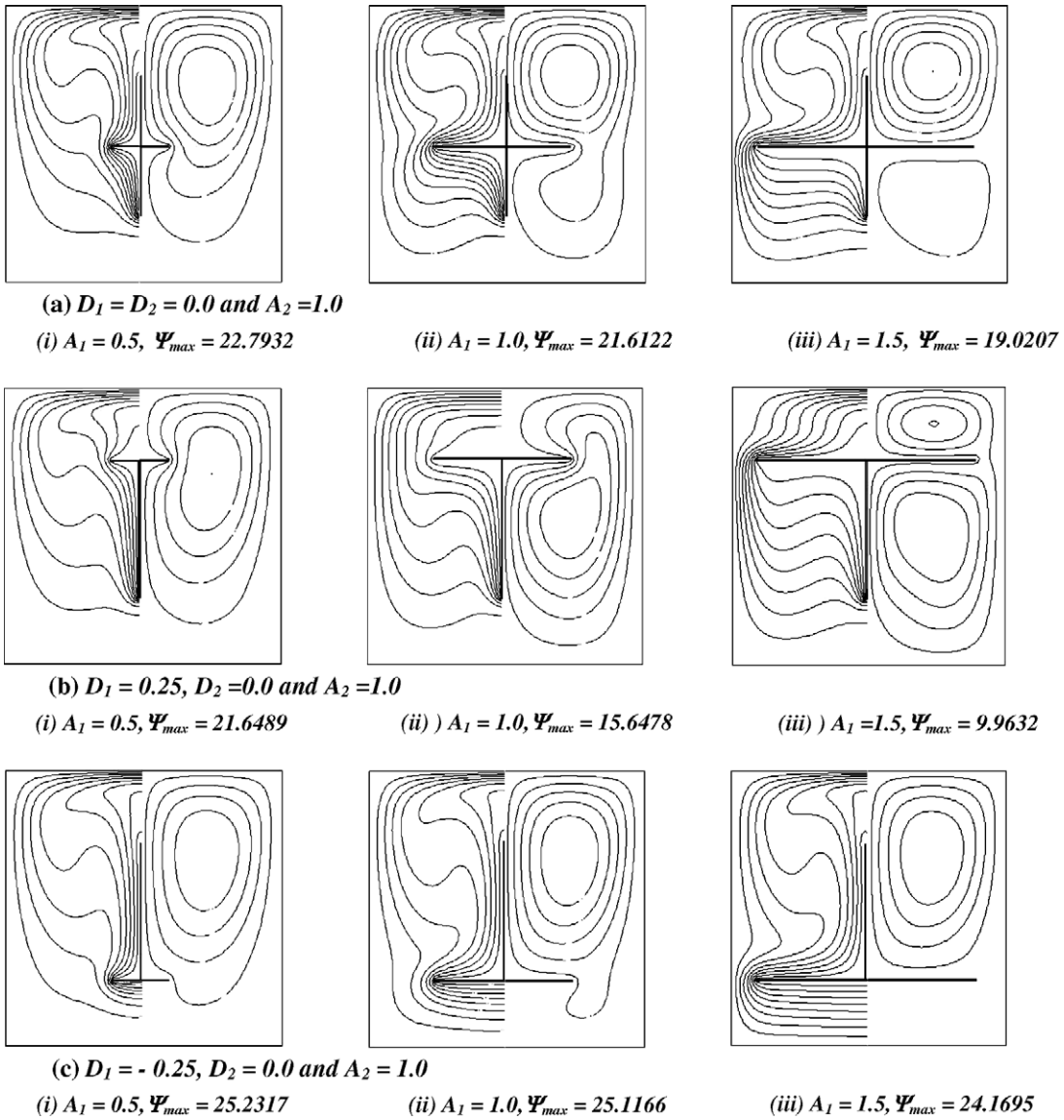


Fig. 4. Isotherms and streamlines for different values of $A_1$ and $D_1$.

of $D_2$ for studying the effect of $A_2$ on the isotherms and streamlines (Fig. 5). We find that the effect is to strengthen convective heat transfer. We also notice that the isotherms get crowded in the vicinity of bottom of the vertical plate for increasing values of $A_2$ and this supplies more energy to the secondary eddies or vortex arising there. Now we discuss the situation when one of the baffles is mounted on a wall. The temperature and flow characteristics for $D_2 = 0.5$ are displayed in Fig. 6. It is observed that an increase in $A_2$ affects the symmetrical thermal emanating from the center of horizontal baffle and hence disturbs the symmetrical streamlines. It makes the left cell to grow in size suppressing the right one and occupy the top of the cavity.

Fig. 7 depicts the extreme cases when both the baffles are wall mounted. Fig. 7a clearly shows the behaviour towards a more stable background state for an increase in $A_1$ as expected. Shown in Fig. 7b is the flow pattern for $D_1 = D_2 = 0.5$. It should be noted that the minimum heat transfer rate was achieved for this configuration among

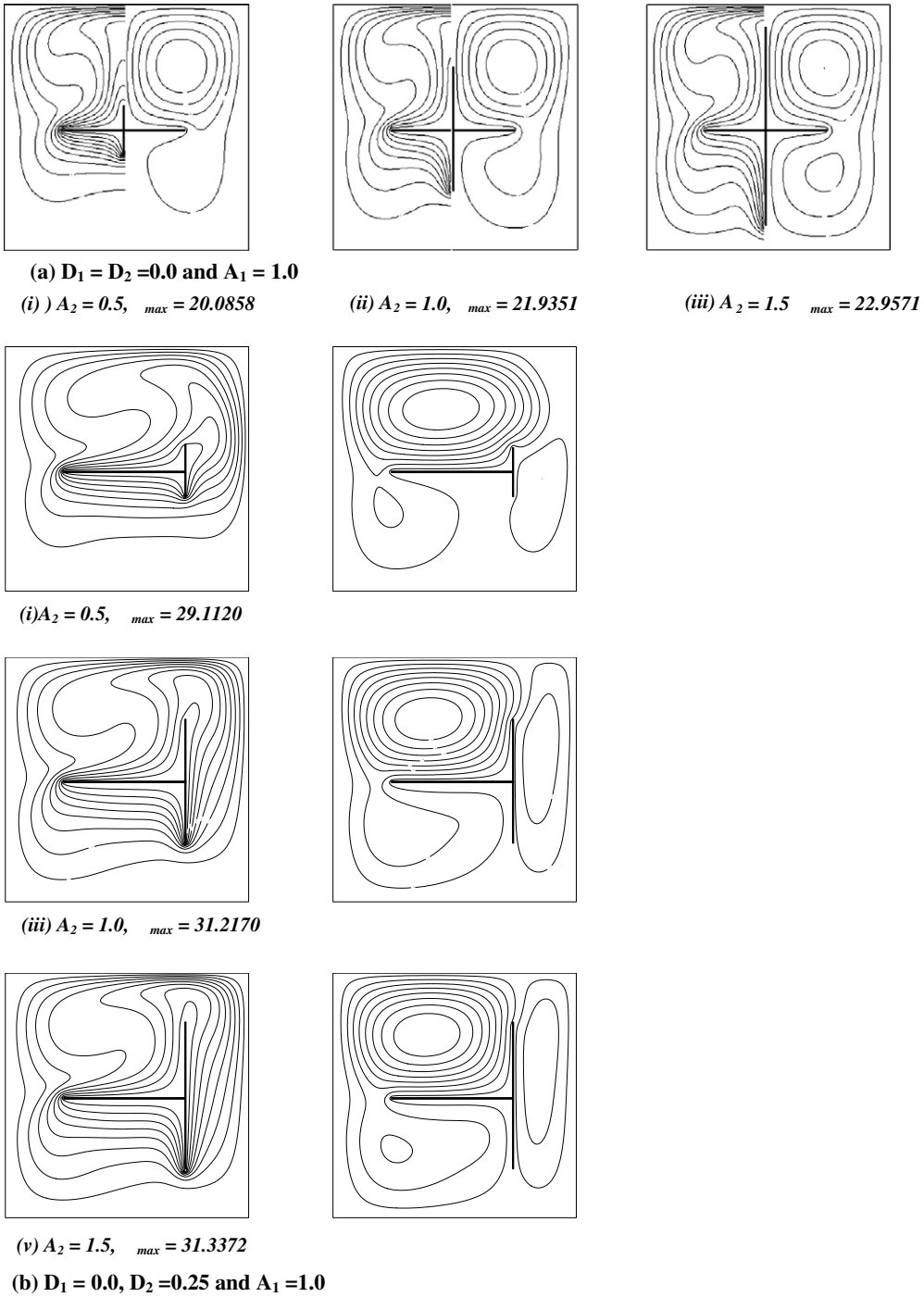


Fig. 5. Isotherms and streamlines for different values of $A_2$ and $D_2$.

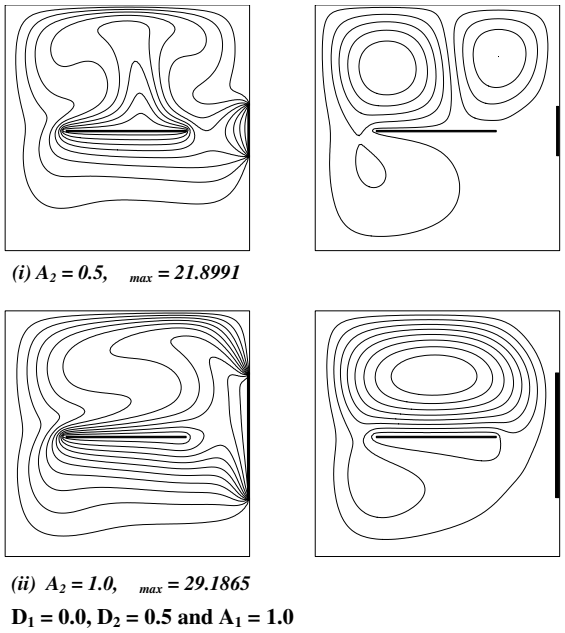


Fig. 6. Isotherms and streamlines for different values of $A_2$.

various locations of the baffles [17]. We notice that the vortex appearing at the top right corner of the cavity for $A_2 = 0.5$ disappears and a single cell pattern with higher momentum is promoted for an increase in $A_2$.

Fig. 8 shows the average Nusselt number for different relative sizes of the heated baffles placed at different locations. In general more amount of fluid is exposed to heat and this proportionately produces large buoyancy force for larger values of both $A_1$ and $A_2$. But at the same time an increase in $A_1$ starts blocking the upward free fluid flow, with a magnitude depending on the position of the horizontal plate (see Fig. 8a) whereas that in $A_2$ no way inhibits vertical flow and thereby promotes large uninterrupted buoyancy force. Similar mechanisms have been recently noticed by Shi and Khodadadi [13]. Thus we observe heat transfer enhancement for an increase in $A_2$ independent of the value of $D_2$ (see Fig. 8b). Let us now see the combined effect of $A_1$ and $D_1$. An examination of Figs. 4c and 8a reveals that conduction effect becomes significant below the horizontal plate and results in higher $\overline{Nu}$ even though there is a slight decrease in $\Psi_{\max}$ for negative values of $D_1$. But when $D_1$ is positive flow inhibition is the only observed phenomena. For example when $A_1$ increases from 0.5 to 1 a less vigorous flow is evident. Shown in the inset of Fig. 8(a) are the wall Nusselt numbers corresponding to $D_1 = 0.5$. This clearly indicates a drop in $Nu_T$ and a substantial increase in wall Nusselt numbers measured at the vertical walls against $A_1$. This is the cause for the fall and then a rise in $\overline{Nu}$ against $A_1$ when $D_1$ is positive.

In order to have a complete understanding we have plotted the average Nusselt number in Fig. 8c when both the baffles are wall-mounted. In general an increase in $\overline{Nu}$ is expected for an increase in $A_2$ for both $D_1 = \pm 0.5$. When $D_1 = 0.5$ and $A_2 = 0$ a stable situation arises in which only

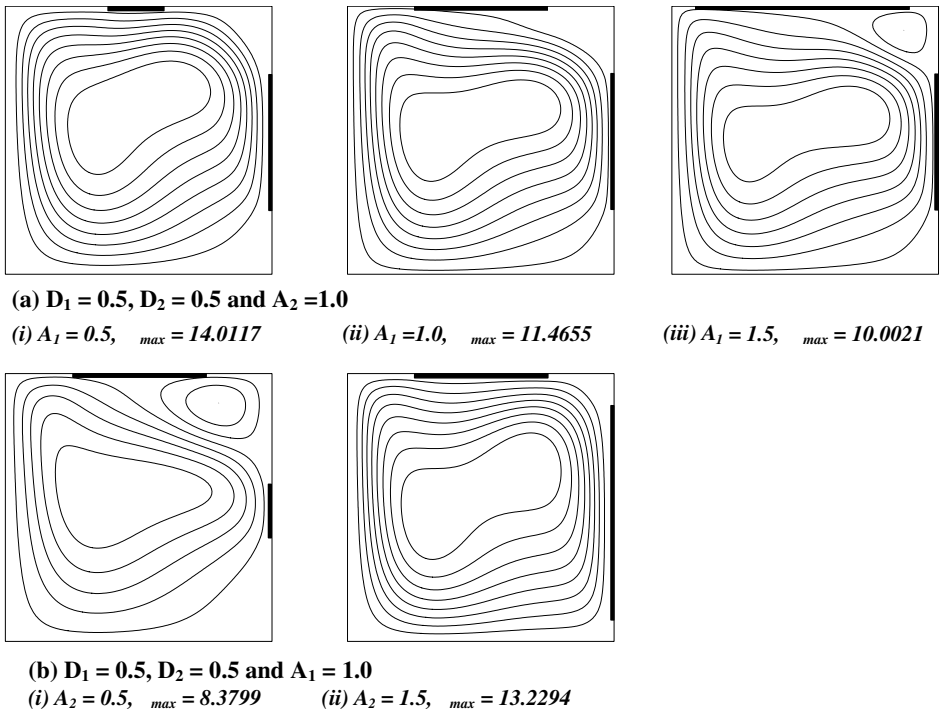


Fig. 7. Streamlines for different values of $A_1$ and $A_2$.

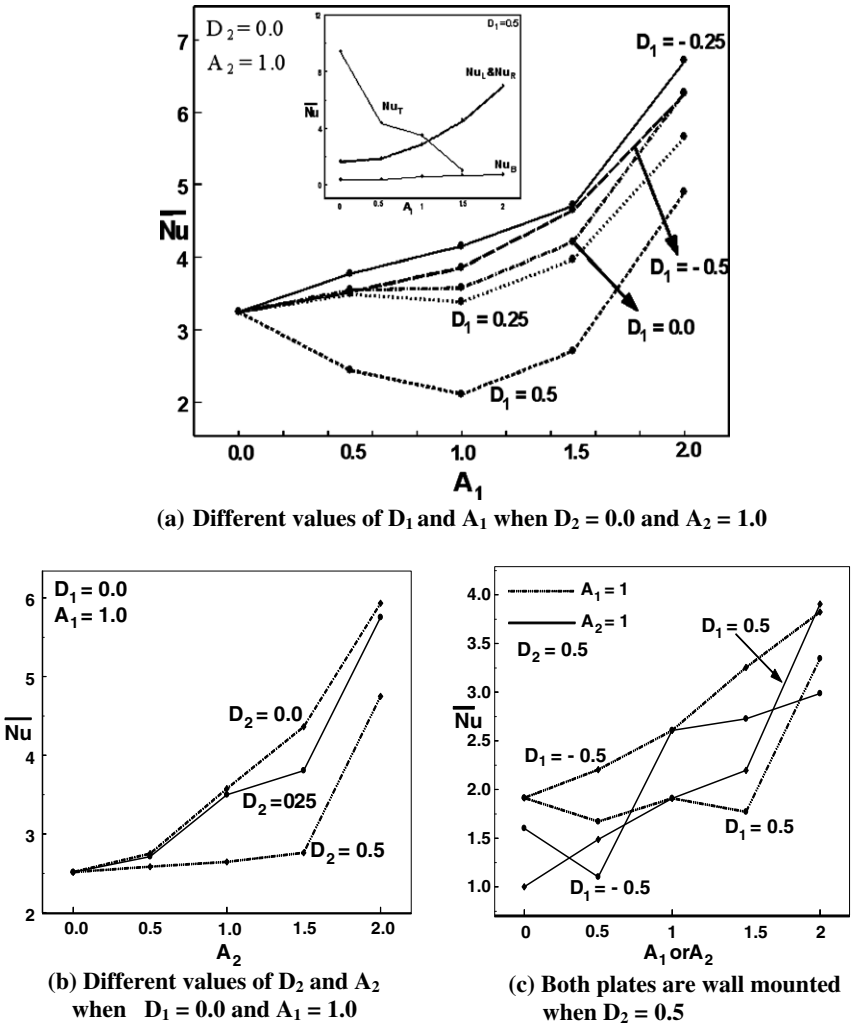


(a) Different values of $D_1$ and $A_1$ when $D_2 = 0.0$ and $A_2 = 1.0$

(b) Different values of $D_2$ and $A_2$ when $D_1 = 0.0$ and $A_1 = 1.0$

(c) Both plates are wall mounted when $D_2 = 0.5$

Fig. 8. Nu for different combinations of $A_1$, $A_2$, $D_1$ and $D_2$.

the conduction mechanism is operative and hence $\overline{Nu}$ is 1. An increase in $A_2$ produces a proportionate increase in the buoyancy force inducing convection. Thus a monotonic increase in $\overline{Nu}$ is observed. But the situation is different when $D_1 = -0.5$ and $A_2 = 0$. Here a pair of well known counter rotating bicellular pattern occurs and the excess heat is removed symmetrically through the surrounding walls. An increase in $A_2$ affects the symmetry in the flow pattern and develops an anticlockwise rotating single cell. But the favourable temperature gradients are not strong enough to allow the cell reaching the top right corner of the cavity for smaller values of $A_2$. This thermally inactive top right corner of the cavity is responsible for a drop in $\overline{Nu}$ when $A_2 = 0.5$.

## 4. Conclusion

Numerical computations were performed to understand buoyancy induced flow and heat transfer inside a square cavity due to two mutually orthogonal isothermal baffles. The baffles were of different sizes and located at various positions within the cavity. The study leads to the following important conclusions.

1. The net heat transfer in the cavity can be enhanced by increasing the vertical baffle length regardless of its position.
2. On the other hand, an increase in the horizontal baffle length can promote heat transfer only when it is located below the center of the cavity.
3. Upward movement of horizontal baffle leads to flow inhibition and hence the average Nusselt number experiences a drop. This effect gets compensated and the average Nusselt number again builds up for large horizontal baffle even when it is located above the center of the cavity.

## Acknowledgements

This work was supported by The Korea Research Foundation and The Korean Federation of Science and Technology Societies Grant funded by Korea Government (MOEHRD, Basic Research Promotion Fund).

## References


[1] W. Nakayama, Thermal management of electronic equipment: a review of technology and research topics, Advances in Thermal Modeling of Electronic Components and Systems, in: A. Bar-Cohen, A.D. Kraus (Eds.), 1 Hemisphere, Washington DC 1988.

[2] G. de Vahl Davis, Laminar natural convection in an enclosed rectangular cavity, Int. J. Heat Mass Transfer 11 (1968) 1675–1693.

[3] Z.Y. Zhong, K.T. Yang, J.R. Lloyd, Variable property effects in laminar natural convection in a square enclosure, ASME J. Heat Transfer 17 (1985) 133–138.

[4] S. Ostrach, Natural convection in enclosure, ASME J. Heat Transfer 110 (1988) 1175–1190.

[5] S. Wakitani, Flow patterns of natural convection in an air-filled vertical cavity, Phys. Fluids 10 (1998) 1924–1928.

[6] S. Saravanan, P. Kandaswamy, Natural convection in low Prandtl number fluids with a vertical magnetic field, ASME J. Heat Transfer 122 (2000) 602–606.

[7] A. Valencia, R.L. Frederick, Heat transfer in square cavities with partially active vertical walls, Int. J. Heat Mass Transfer 32 (1989) 1567–1989.

[8] P.K.B. Cho, H. Ozoe, S.W. Churchill, N. Lior, Laminar natural convection in an inclined rectangular box with the lower surface half-heated and half-insulated, ASME J. Heat Transfer 105 (1983) 425–432.

[9] M. Ciofalo, T.G. Karayiannis, Natural convection heat transfer in a partially or completely – partitioned vertical rectangular enclosure, Int. J. Heat Mass Transfer 34 (1991) 167–179.

[10] R.L. Frederick, A. Valencia, Heat transfer in square cavities with a conducting partition on its hot wall, Int. Commun. Heat Mass Transfer 16 (1989) 347–354.

[11] M. Keyhani, L. Chen, D.R. Pitts, The aspect ratio effect on natural convection in an enclosure with protruding heat source, ASME J. Heat Transfer 113 (1991) 883–891.

[12] S.T. Tasnim, M.R. Collins, Natural analysis of heat transfer in a square cavity with baffle on the hot wall, Int. Commun. Heat Mass Transfer 31 (2004) 639–650.

[13] X. Shi, J.M. Khodadadi, Laminar natural convection heat transfer in a differentially heated square cavity due to a thin fin on the hot wall, ASME J. Heat Transfer 125 (2003) 624–634.

[14] H.F. Oztop, I. Dagtekin, A. Bahloul, Comparison of position of a heated thin plate located in a cavity for natural convection, Int. Commun. Heat Mass Transfer 31 (2004) 121–132.

[15] I. Dagtekin, H.F. Oztop, Natural convection heat transfer by heated partitions within enclosure, Int. Commun. Heat Mass Transfer 28 (2001) 823–834.

[16] E. Papanicolaou, Y. Jaluria, Mixed convection from simulated electronic components at varying relative positions in a cavity, ASME J. Heat Transfer 116 (1994) 960–970.

[17] T. Icoz, Y. Jaluria, Design of cooling systems for electronic equipment using both experimental and numerical inputs, ASME J. Electronic Packaging 126 (2004) 465–471.

[18] S. Saravanan, P. Kandaswamy, A.K. Abdul Hakeem, J. Lee, Buoyancy convection in a cavity with mutually orthogonal heated plates, ASME J. Heat Transfer, submitted for publication.